TECHNICAL REPORT STANDARD PAGE

1. Title and Subtitle

Stabilizing Blended Calcium Sulfate (BCS) Using Biologically-Mediated Method for Application in Base Course

2. Author(s)

Noura Saleh; Hai Lin

3. Performing Organization Name and Address

Department of Civil and Environment Engineering
Louisiana State University
3255 Patrick F. Taylor Hall
Baton Rouge, LA, 70810

4. Sponsoring Agency Name and Address

Louisiana Department of Transportation and Development
P.O. Box 94245
Baton Rouge, LA 70804-9245

5. Report No.

FHWA/LA.17/Enter 3-digit Report No.

6. Report Date

Enter Report date

7. Performing Organization Code

LTRC Project Number: 20-5 TIRE
SIO Number: DOTLT 1000-302

8. Type of Report and Period Covered

Final Report
Enter Date: Month/Year – Month/Year

9. No. of Pages

Enter number of pages

10. Supplementary Notes

Conducted in Cooperation with the U.S. Department of Transportation, Federal Highway Administration

11. Distribution Statement

Unrestricted. This document is available through the National Technical Information Service, Springfield, VA 21161.

12. Key Words

Blended calcium sulfate, Cementation; Enzyme induced carbonate precipitation; Microbially induced carbonate precipitation.

13. Abstract

Blended calcium sulfate (BCS) is a recycled flurogypsum waste material mixed with lime. Approximately 90,000 metric tons of flurogypsum are generated annually in the United States, posing a serious disposal problem to the environment. The Louisiana Department of Transportation and Development (LA DOTD) has been using BCS as an alternative road base material for almost three decades. Long-term field tests showed that BCS has a satisfactory performance in dry areas. However, its moisture susceptibility problem has resulted in the strength degradation of BCS in a wet environment.

In order to eliminate this issue, this study focuses on investigating the feasibility of utilizing the biologically-mediated soil improvement methods (e.g., microbially induced carbonate precipitation (MICP) and enzyme induced carbonate precipitation (EICP)) to stabilize BCS. MICP utilizes natural soil bacteria to hydrolyze urea (nitrogenous waste) as a nutrient source and produce $CaCO_3$ cementation. EICP uses a free urease enzyme to catalyze the hydrolysis of the urea producing $CaCO_3$ in the presence

of calcium ions. The mechanical behavior of BCS treated with both methods was investigated by monitoring the shear wave (S-wave) velocity during the MICP and EICP treatments and measuring unconfined compressive strength. Microscale imagining, including Scanning Electron Microscope (SEM) and Energy Dispersive Spectroscopy (EDS), X-Ray Diffraction (XRD), and Raman analysis were presented to investigate the micro-scale characteristics of the treated and untreated BCS samples.

The testing results showed that MICP and EICP treatments were not effective for stabilizing BCS due to the several inhibiting factors related to the chemical properties of BCS.

Project Review Committee

Each research project will have an advisory committee appointed by the LTRC Director. The Project Review Committee is responsible for assisting the LTRC Administrator or Manager in the development of acceptable research problem statements, requests for proposals, review of research proposals, oversight of approved research projects, and implementation of findings.

LTRC appreciates the dedication of the following Project Review Committee Members in guiding this research study to fruition.

LTRC Administrator/Manager

[Enter name]

[Enter field of research]Research Manager

Members

Enter member's names, one per line

Directorate Implementation Sponsor

Christopher P. Knotts, P.E.

DOTD Chief Engineer

Stabilizing Blended Calcium Sulfate (BCS) Using Biologically-Mediated Method for Application in Base Course

By
Noura Saleh
Graduate Research Assistant
Hai Lin
Assistant Professor

Department of Civil and Environment Engineering
Louisiana State University
3255 Patrick F. Taylor Hall, Baton Rouge, LA 70803

LTRC Project No. 20-5 TIRE
SIO No. DOTLT 1000-302

conducted for
Louisiana Department of Transportation and Development
Louisiana Transportation Research Center

May 2020

Abstract

Blended calcium sulfate (BCS) is a recycled flurogypsum waste material mixed with lime. Approximately 90,000 metric tons of flurogypsum are generated annually in the United States, posing a serious disposal problem to the environment. The Louisiana Department of Transportation and Development (LA DOTD) has been using BCS as an alternative road base material for almost three decades. Long-term field tests showed that BCS has a satisfactory performance in dry areas. However, its moisture susceptibility problem has resulted in the strength degradation of BCS in a wet environment.

In order to eliminate this issue, this study focuses on investigating the feasibility of utilizing the biologically-mediated soil improvement methods (e.g., microbially induced carbonate precipitation (MICP) and enzyme induced carbonate precipitation (EICP)) to stabilize BCS. MICP utilizes natural soil bacteria to hydrolyze urea (nitrogenous waste) as a nutrient source and produce $CaCO_3$ cementation. EICP uses a free urease enzyme to catalyze the hydrolysis of the urea producing $CaCO_3$ in the presence of calcium ions. The mechanical behavior of BCS treated with both methods was investigated by monitoring the shear wave (S-wave) velocity during the MICP and EICP treatments and measuring unconfined compressive strength. Microscale imagining, including Scanning Electron Microscope (SEM) and Energy Dispersive Spectroscopy (EDS), X-Ray Diffraction (XRD), and Raman analysis were presented to investigate the micro-scale characteristics of the treated and untreated BCS samples.

The testing results showed that MICP and EICP treatments were not effective for stabilizing BCS due to the several inhibiting factors related to the chemical properties of BCS.

Acknowledgments

The investigators appreciate the Louisiana Transportation Research Center (LTRC) for funding this project through the Transportation Innovation for Research Exploration (TIRE) Program. The authors would like to acknowledge Dr. Doc Zhang for his assistance on acquiring blended calcium sulfate. The authors would also like to acknowledge the help, guidance, and administrative direction provided to them by Dr. Vijaya Gopu, Associate Director of LTRC.

Implementation Statement

MICP and EICP treatments have several potential advantages for BCS stabilization. Since these two treatment processes do not involve hydration reactions, their processes will not cause volume expansion in BCS. Furthermore, MICP and EICP utilize natural soil bacteria and enzyme, urea (nitrogenous waste from the urine of mammals), and Ca^{2+} (BCS can partially provide a source of Ca^{2+}) to produce calcite cementation, which will have the great potential to reduce the material cost for BCS stabilization. If success, this research will have the potential to offer LA DOTD a natural alternative to stabilize BCS material for base course construction, advancing the applications of BCS.

Based on the results reported, using MICP and EICP solutions is not an effective method for stabilizing BCS due to the presence of SO_4^{2-} and low pH of BCS that inhibit $CaCO_3$ precipitation. However, MICP and EICP could be effective for other geotechnical related applications, including sealing soil cracks on embankment slopes, ground improvement, and pile post-grouting [1], which is currently under investigation by the research team.

Table of Contents

List of Tables

List of Figures

Introduction

Biologically-mediated soil improvement is an innovative ground improvement method that could be suitable for many geotechnical engineering problems [2] [3] [4] [5]. The promising bio-mediated improvement methods include Microbially Induced carbonate Precipitation (MICP) and Enzyme Induced Carbonate Precipitation (EICP). MICP is a metabolic process of natural bacteria to hydrolyze urea as a nutrient source and produce calcium carbonate ($CaCO_3$) precipitation within the soil matrix [6] [7]. The most common microorganism employed for MICP is *Sporosarcina Pasteurii* (ATCC 11859), which can produce urease to hydrolyze urea into ammonium and carbonic acid with increasing alkalinity. This alkaline environment and the increasing availability of carbonate ion shifts the equilibrium of $CaCO_3$ dissolution/precipitation toward precipitation. EICP uses free urease enzyme rather than microbial urease (used in ureolytic MICP) to catalyze urea hydrolysis and induce $CaCO_3$ precipitation [8] [9] [10]. The precipitated $CaCO_3$ coat soil particles, cement the soil matrix, and fill the soil void space, increasing strength, stiffness, and dilatancy [11] [12] [13] [14] [15] [10].

Blended calcium sulfate (BCS) is a recycled flurogypsum waste material mixed with lime. Approximately 90,000 metric tons of flurogypsum are generated annually in the United States, posing a serious disposal problem to the environment. The Louisiana Department of Transportation and Development (LA DOTD) has been using BCS in pavement construction on a trial basis over the last 15 years [16]. While this material has performed satisfactorily on many projects, its moisture sensitivity has concerned LA DOTD engineers. This moisture sensitivity often results in construction difficulties in a wet environment and sometimes failures of pavements due to strength deterioration. Researchers have been searching for ways to stabilize BCS using Portland cement. However, ettringite is produced when stabilizing BCS with Portland cement, which is responsible for detrimental expansion and strength deterioration of BCS. Granulated ground blast furnace slag (GGBFS) was also used to stabilize BCS, the unconfined compression strength for GGBFS-stabilized BCS increased significantly. However, the GGBFS-stabilized BCS did not obtain adequate early strength due to the slow reactivity of GGBFS [17]. In order to improve the early strength of the GGBFS-Stabilized BCS, Tao and Zhang [17] explored some secondary cementation materials into the GGBFS-stabilized BCS, including lime, cement, and fly ash. Although the results of using GGBFS and secondary cementation materials were promising, it was not a cost-effective way to stabilize BCS [17]. The objective of this research is to investigate the feasibility of

stabilizing BCS using MICP and EICP to overcome volume expansion and water sensitivity problems.

Literature Review

Blended calcium sulfate (BCS) is a recycled fluorogypsum (FG) blended with 2%–5% of alkali materials such as lime or circulating fluidized bed combustion (CFBC) ash. Lime and CFBC are used for adjusting the pH of FG. The recycled fluorogypsum is generated during the production of hydrofluoric acid from fluorspar. It is discharged in a slurry state and solidified into a dry state in holding ponds after water evaporation [18].

The Louisiana Department of Transportation and Development (LA DOTD) has been using BCS as a base course in pavement construction on a trial basis over the last 15 years. LA DOTD engineers found that moisture content and dry unit weight affect the strength of raw BCS. The properties of BCS passing through sieve No. 4 (opening size of 4.75 mm) were investigated. The specific gravity of BCS is 2.38, which is lighter than naturally occurring aggregates, such as sand or gravel. BCS has a pH of 6.5, and its chemical components are listed in Table 1 [17]. Unconfined compression tests were used to investigate the unconfined compressive strength (UCS) of BCS with different water contents [17]. Figure 1 shows that the UCS at a moisture content of 2% dropped rapidly to one-fifth of the unconfined compressive strength of the dry BCS. Figure 1 also suggests that using BCS as a base material for constructing pavements is inappropriate as the strength of BCS will decrease significantly under wet conditions [19].

In order to use BCS as a base material for pavements, different cementing agents were tested to improve the strength deterioration of BCS under wet conditions. Portland cement is a widely-used cementing agent, while it was not suitable to stabilize BCS because stabilizing gypsum by Portland cement is accompanied by ettringite production [20]. The production of the ettringite is often responsible for volume expansion of stabilized BCS that leads to strength deterioration. Mixing the Portland cement with silica fume could stabilize gypsum without experiencing any volume expansion [20] [21]. However, it is not a cost-competitive solution due to the relatively high cost of silica fume. Ground granular blast furnace slag (GGBFS) with a grade 120 was used as an inexpensive cementing agent to stabilize BCS with 10% by mass. The ratio of UCS for GGBFS-stabilized BCS between wet and dry states reached 0.83 after 28 days. However, the BCS stabilized with GGBFS did not achieve an early strength due to the slow reactivity of GGBFS. Secondary cementation material such as type I Portland cement, lime, or class C fly ash, was added to GGBFS-stabilized BCS to enhance the early strength of the mix. The highest UCS after 7 days was BCS-GGBFS-cement with a ratio

of 91:7.5:1.5 by weight. Class C fly ash was excluded as it caused a higher volume expansion. The effectiveness of all the above methods (e.g., Portland cement with silica fume, GGBFS, and GGBFS mixed with another cementing agent) to stabilize the BCS was also evaluated from the perspective of water resistance, strength, volumetric expansion. Although some methods were successful (e.g., BCS-GGBFS-cement), a cheaper and environmentally friendly method is still lacking for stabilizing BCS. This study uses bio-cementation to stabilize BCS and investigates the effects of bio-cementation on the mechanical behavior of BCS.

Table 1. Chemical Composition of BCS under Investigation [17]

Compositions	**Percentage by mass**
SiO_2	0.5
Al_2O_3	0.1
Fe_2O_3	0.2
CaO	29.0
SO_4	54.0
CO_2	3.0
H_2O	5.0-30.0

The FG has also been investigated as a construction material for outdoor and underwater applications [22]. Compared to the Portland cement, FG has several advantages, including lower unit weight, lower cost of the production, and the availability of fluorogypsum in Louisiana [22]. pH-adjusted FG for outdoor and underwater applications is prepared by circulating fluidized bed combustion (CFBC) ash (an alkali material) for neutralizing the FG. A sample of pH-adjusted FG using CFBC was analyzed using XRD to investigate the crystal composition, and it showed (G: $CaSO_4.2H_2O$), anhydrite (A: $CaSO_4$), fluorite (F: CaF_2), and quartz (Q: SiO_2). pH-adjusted FG for outdoor and underwater applications was investigated by considering different proportions of dry components of pH-adjusted fluorogypsum (FG), fly ash (FA), and Portland cement (PC). The compressive strength decreased considerably with increasing content of pH-adjusted FG when the PC content is equal to 2% and 6%. However, its decrease is less pronounced

for PC content equal to 10% by weight. The maximum compressive strength, for a different amount of PC, was achieved at pH-adjusted FG content of 60%, but the minimum compressive strength was attained at pH-adjusted FG content of 90%. Bigdeli concluded that a mixture of 62% pH-adjusted FG, 35% fly ash (FA), and 3% Portland cement (PC) by weight, was successfully achieved for stabilizing FG and eliminating the volume expansion for outdoor and underwater applications.

Figure 1. Relationship between UCSs and moisture contents of BCS [17]

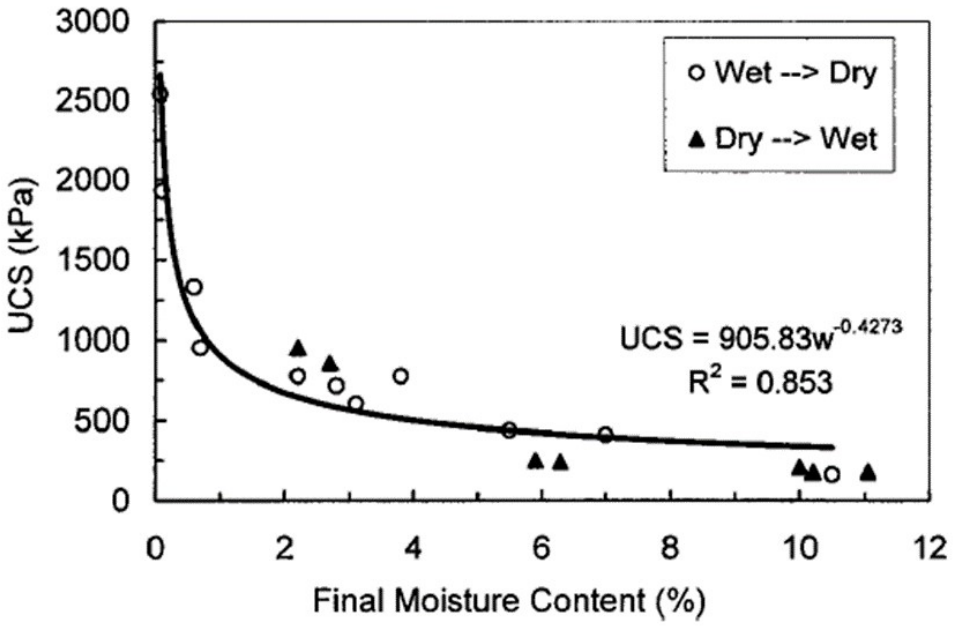

MICP is a microbially regulated process of $CaCO_3$ precipitation that can be induced by microbial-catalyzed hydrolysis of urea (ureolysis) [6] MICP uses natural bacteria (*Sporosarcina Pasteurii*) to hydrolyze urea by their urease enzyme into ammonium and carbonic acid, which increases the alkalinity (pH=~9) of the surrounding environment. This alkaline environment and the increasing availability of carbonate ion shifts the equilibrium of $CaCO_3$ dissolution/precipitation towards precipitation [6] [2] [3]. The resulted reaction is shown below:

$$CO(NH)_2 + 2H_2O + CaCl_2 = CaCO_3\downarrow + 2NH_4Cl$$

The precipitated $CaCO_3$ cements the sand matrix and fills the soil pore space, increasing its strength and stiffness and decreasing the hydraulic conductivity [7] [11] [23] [13] [14]. Research on MICP has explored potential applications including ground improvement for

liquefaction mitigation, coastal and desert sand stabilization, seepage and erosion control, coal ash stabilization, and scour mitigation [5] [24] [25] [26] [27] [28] [29] [30] [31] [32] [33].

EICP uses a free urease enzyme rather than microbial urease (used in ureolytic MICP) to catalyze urea hydrolysis and induce $CaCO_3$ precipitation [8] [9] [10]. As such, EICP does not require nutrients for bacterial cultivation, oxygen to sustain aerobic ureolytic bacteria, or consideration of the competing effect of other microorganisms [34] [9]. A typical application of EICP requires fewer chemicals compared to MICP. Specifically, neither ammonium chloride (NH_4Cl) nor nutrient broth is needed with EICP. The small size of urease (~12 nm) allows EICP to penetrate silt-sized soil, while the larger size of bacterial cells (~1 μm) prevents MICP media from entering these fine-grained soils.

The small size of the urease enzyme in EICP will result in a more uniform distribution of $CaCO_3$ than that of MICP. Although the uniformity of $CaCO_3$ can be achieved by the EICP treatment, the treatment using MICP can precipitate an additional amount of $CaCO_3$ for the same sample under the same conditions of treatment. Furthermore, MICP-treated samples showed higher strength than EICP treated samples [35]. This is probably because enzymes cannot attach to soil particles and do not act as nucleation sites in the $CaCO_3$ precipitation process, which resulted in different precipitation patterns and crystal shapes of $CaCO_3$ between MICP and EICP treatments [35].

Objective

The goal of this project is to explore the use of bio-mediated soil improvement methods (MICP and EICP) to stabilize BCS for application in base course construction. MICP and EICP hydrolyze urea (the nitrogenous waste in the urine of mammals) as a nutrient source and produce $CaCO_3$ cementation within the soil matrix. MICP and EICP treatment processes have been shown to improve the behavior of the soil matrix by increasing its strength and stiffness. These treatment processes can be used to stabilize BCS, which will reduce the volume expansion of BCS, stiffen BCS quickly to achieve higher early strength, reduce its moisture susceptibility, and ultimately improve the long-term performance of stabilized BCS.

Scope

In order to develop suitable MICP and EICP treatment methods and investigate the effectiveness of using MICP and EICP for BCS stabilization, the following tasks are proposed.

- Monitor the S-wave velocities during MICP and EICP treatments to investigate the increase of stiffness of BCS specimens.
- Investigate the consolidation behavior of MICP-treated BCS specimens to assess how much the specimens can deform.
- Perform unconfined compression tests for MICP-and EICP-treated specimens to measure the unconfined compressive strength (UCS).
- Measure the $CaCO_3$ content of each specimen to assess the performance of MICP and EICP treatments.
- Perform microscale analysis using Scanning Electron Microscope (SEM), Energy Dispersive Spectroscopy (EDS), X-Ray Diffraction (XRD), and Raman spectrum to investigate the morphology and characteristics of BCS samples.

Methodology

1. Equipment

Two types of cells (stainless steel and acrylic) with different dimensions were used to prepare the specimens. Stainless steel cell was used for monitoring the shear wave (S-wave) velocity of the BCS specimen during MICP and EICP treatments. The acrylic cell was used for preparing the BCS specimens for unconfined compression tests. The S-wave velocity was also monitored in the acrylic cell.

a. Stainless Steel Cell

Figure 2 shows the setup of the stainless-steel cell with an inner diameter of 2.5 inches and a height of 2.19 inches. The cell was positioned in a consolidation test load frame to measure the S-wave velocity and the settlement of the specimen under loading and unloading conditions. Two S-wave sensors (bender elements) were installed in the top and bottom plates of the cell for measuring the S-wave velocity during the MICP and EICP treatments. Bender elements were fabricated in-house using Piezo element (4 × 8 mm parallel type-PSI-5H4E T226-H4-303Y from Piezo Systems). A data acquisition system was connected to the bender elements, as shown in Figure 3. The data acquisition system consists of a function generator, filter, amplifier, and digital oscilloscope. A 2 V square wave with 100 Hz was used for signal input. The received signal was filtered through a filter-amplifier (low-pass filter at f =30 kHz and high-pass filter at f =100 Hz) to reduce noncoherent noise [36]. The travel time of the S-wave was shown on a digital oscilloscope. The shear wave velocity (V_s) was determined by dividing the tip to tip distance (L) by the travel time (t) using the first arrival point of the wave [36].

b. Acrylic Cell

A fabricated acrylic cell with a diameter of 2.83 inches and a height of 8 inches was used for preparing the samples for the unconfined compression test. Two bender elements were installed in the top and bottom plates of the cell for measuring S-wave velocity during the treatment. The cell was positioned under a fabricated load frame as shown in Figure 4. After MICP and EICP treatments,

unconfined compression tests were performed using a Geo-Jack unconfined compression system as shown in Figure 5.

c. Rapid Carbonate Analyzer for $CaCO_3$ Content Measurement

A rapid carbonate analyzer (shown in Figure 6) was used for $CaCO_3$ content measurement. Measurement procedure followed the ASTM standard (ASTM D4373-14) [37].

Figure 2. Setup of the stainless-steel cell for consolidation tests.

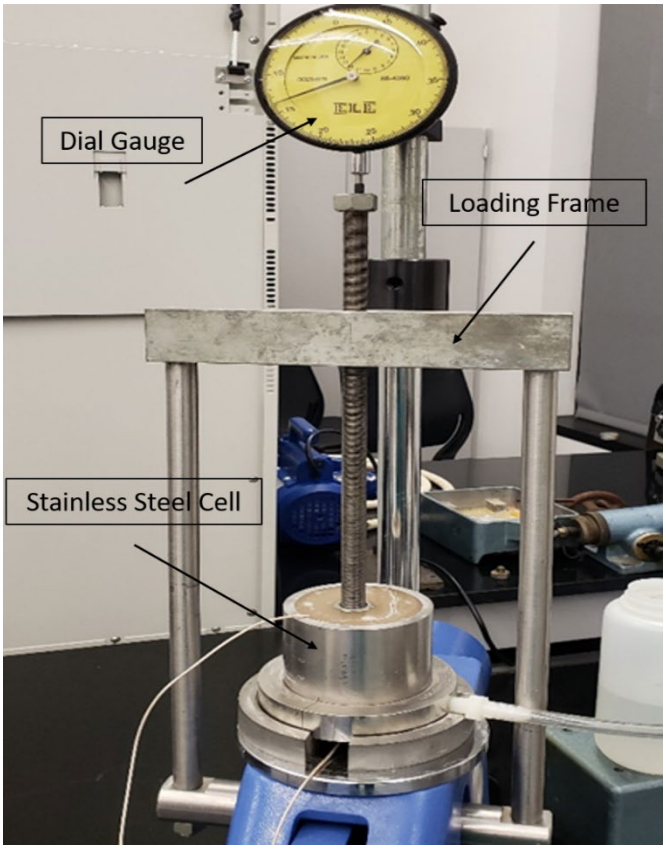

Figure 3. Data acquisition system of S-wave velocity measurements.

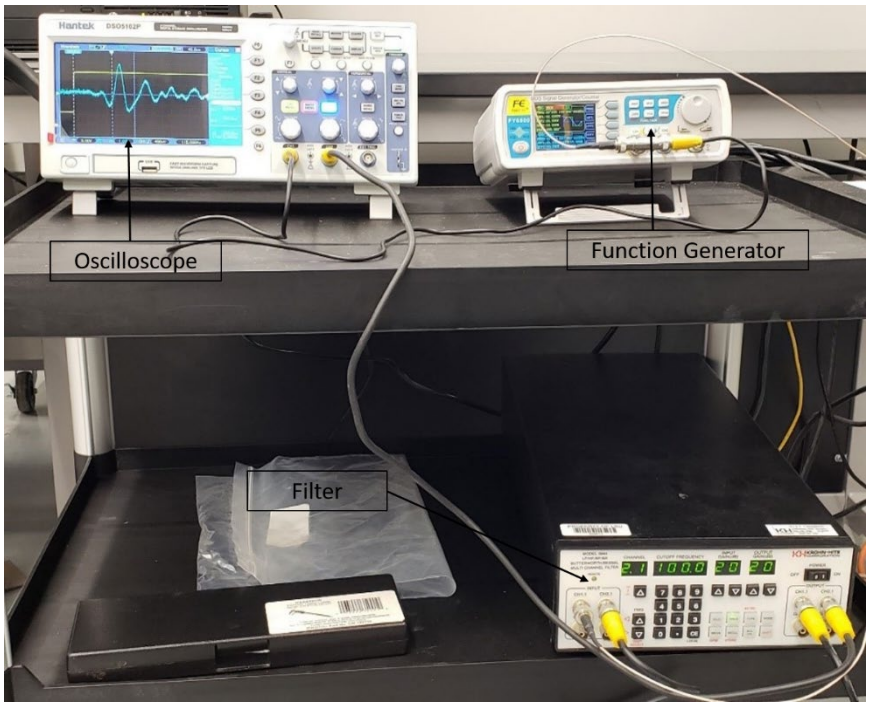

Figure 4. Setup of the Acrylic sample cell.

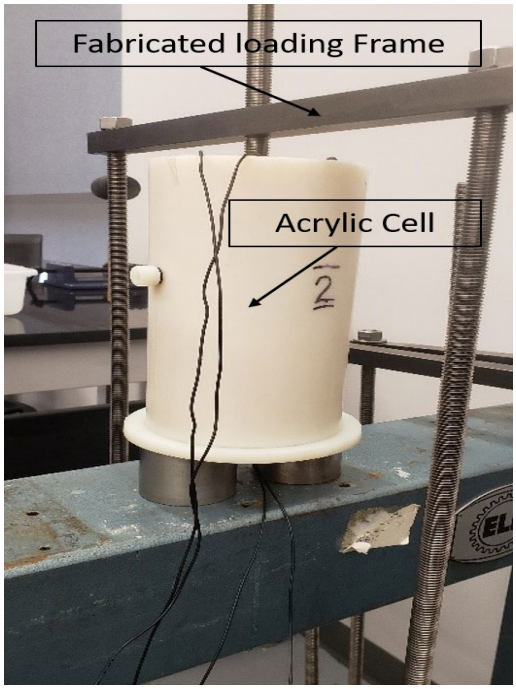

Figure 5. Unconfined compression test device.

Figure 6. The chamber for rapid determination of carbonate content.

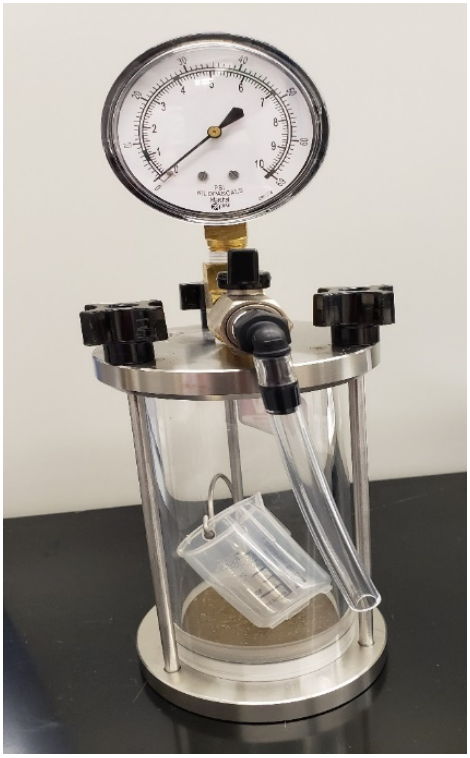

2. Materials

a. Bacteria Preparation and MICP Solutions

The gram-positive bacteria, *Sporosarcina pasteurii* (ATCC 11859), was used in MICP treatment. The bacterial cultures were grown in a growth media solution shown in Table 2 for 24 hours, then harvested and stored in 15% glycerol at −86°C to maintain a uniform bacterial stock for future use. The stock culture of *Sporosarcina pasteurii* was used to grow in the growth media again in an incubator shaker at 170 rpm, 30ºC for approximately 24 hours until OD_{600}=0.8~1.2 (OD_{600}: optical density of a sample measured at a wavelength of 600 nm). Then, the bacteria were harvested and centrifuged twice at 4000 g for 30 minutes to target bacteria density 1×10^{8} cells/ml, the bacteria were stored in 4ºC refrigerator until further use. Table 2 also presents the chemical components of the urea medium and cementation medium that were used in MICP treatment for BCS samples [23].

b. EICP Solutions

The enzyme induced carbonate precipitation (EICP) treatment solutions were prepared by dissolving calcium chloride dehydrate ($CaCl_2.2H_2O$), urea, urease enzyme, and non-fat milk. Table 3 shows three different solutions used in EICP treatment [38].

c. Blended Calcium Sulfate

BCS was prepared by passing through sieve No. 4. The specific gravity of BCS passing No. 4 sieve was determined to be 2.38. Figure 7 shows the particle size distribution of BCS with a uniformity coefficient C_u=150 and a coefficient of curvature C_c=24 [17]. The compaction curves of BCS under standard and modified compaction energies are shown in Figure 8, which indicates the maximum dry unit weight is 15.78 kN/m^3 (100.5 pcf) with the optimum water content of 12% for the standard Proctor procedure [17].

Table 2. Summary of MICP solutions.

Solution	Constituents
Tris buffer	7.6 g Tris hydrochloric acid 54.7 g Tris base in 500 mL distilled water
Growth medium	10 g Yeast extract 5 g Ammonium sulfate in 500 mL of 0.13 M Tris buffer (pH 9.0) Sterilized by filter
Urea medium	20 g/L Urea 2.12 g/L $NaHCO_3$ 20 g/LNH_4CL 3 g/L Bacto nutrient broth Adjust the pH of the medium to 6.0 with 5 M HCL sterile filtration
Cementation medium	Urea medium constituent 0.3 M $CaCl_2$

Table 3. Summary of EICP solutions.

EICP Solution #1	EICP Solution #2	EICP Solution #3
0.67 M $CaCl_2$	0.67 M $CaCl_2$	0.67 M $CaCl_2$
1 M Urea	1 M Urea	1 M Urea
3 g/L enzyme	3 g/L enzyme	_
4 g/L non-fat milk powder	_	_

Figure 7. Particle Size Distribution of BCS [17]

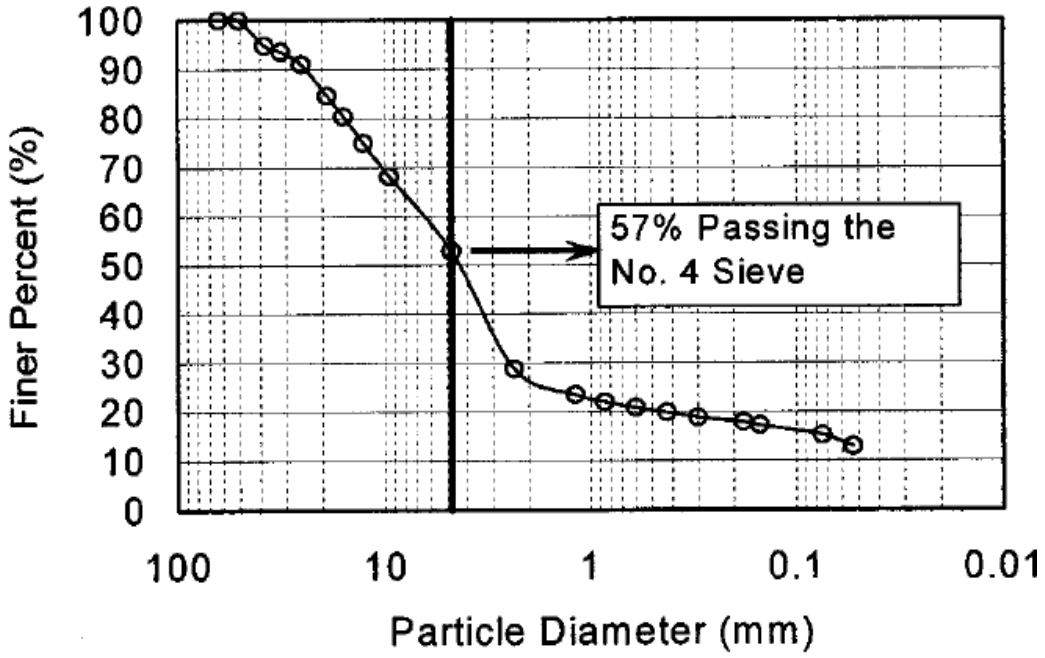

Figure 8. Compaction Curves of BCS [17]

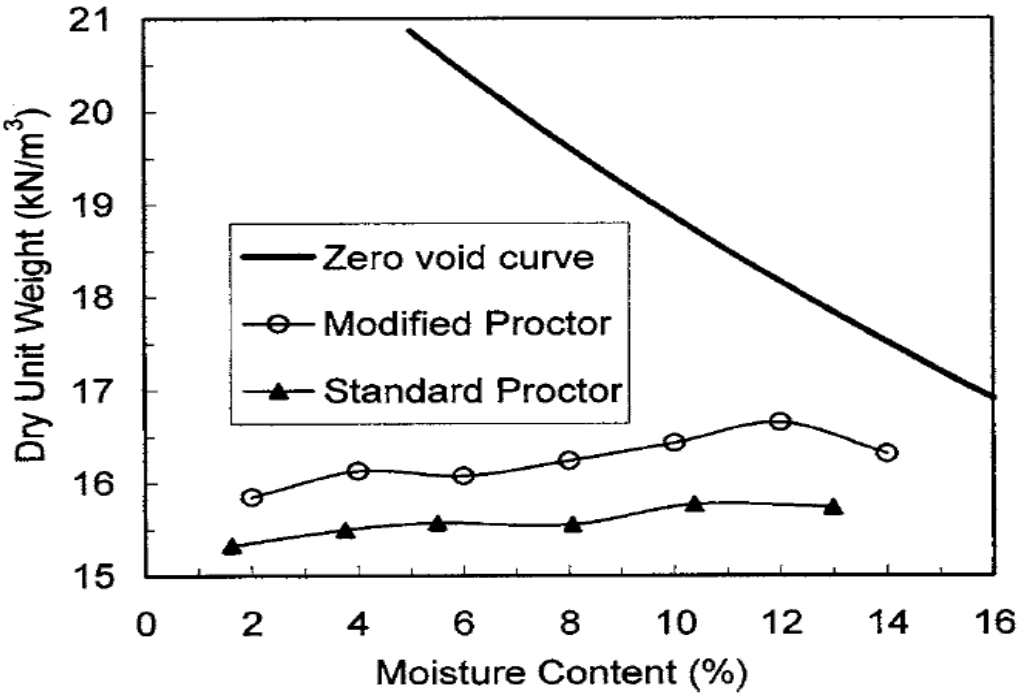

3. Experimental Procedure

a. MICP Treatment

I. Sample preparation

Specimens in stainless-steel cell were 2.5 inches in diameter and 1 inch in height. Specimens were prepared by mixing BCS with MICP solutions to target an average density of 96.1 pcf. 124.3 g (0.27 lb) of BCS was mixed with 30 mL of one of four MICP solutions as shown in Table 4. The mixtures were poured into the cell in three equal layers. Every layer was compacted to make sure that the air was squeezed out from the specimen. After placing the mixtures, the top cap was then placed on the sample. The load frame was installed on the top cap to apply a 10 kPa load. The specimens were cured for two days to precipitate $CaCO_3$. After two days, the loading and unloading schemes were applied to the specimens to investigate the consolidation behavior of MICP-treated BCS. S-wave velocities of the specimens were also monitored during the MICP treatment and loading and unloading.

Specimens in the acrylic cell were 2.8 inches in diameter and 6 inches in height. To target dry density 96.1 pcf, 957.7 g (2.1 lb) of BCS was mixed with 230 ml of one of the MICP solutions shown in Table 4. The specimens were prepared with the same procedure as the specimens for stainless-steel cell.

II. Loading and unloading

After two days of MICP treatment, loading stress was increased to 50, 100, 200, 300, 400, 500, 600, 700, 800, 900, 1000, 1100, and 1200 kPa and then decreased using the same values. Each loading and unloading period lasted for 15 min as recommended by [39]. S-wave velocity and displacement were measured using bender elements and dial gauge by the end of every loading or unloading stage.

III. S-wave Velocity

Bender elements installed in the cell were connected to the data acquisition system after sample preparation. The time difference readings were recorded every 15 minutes during MICP and EICP treatments. After the first three hours of treatment,

the time difference was recorded every 12 hours. The S-wave velocity was measured according to the equation shown below.

$$V_S = L / t$$

Where V_S is the shear wave velocity, L is the distance from the tip to tip of bender elements, and t is the time difference.

During loading and unloading stages, S-wave velocity was measured by the end of every loading or unloading stage.

IV. Unconfined compression test

After preparing the mixture of BCS and MICP solutions in the acrylic cell, specimens were cured for seven days under MICP treatment. After curing, specimens were extruded from the cell and dried in air for one day. Some specimens were dried in air for three days and then were transferred to the oven to dry for four additional days. The unconfined compression tests were carried out at a constant rate of 1 %/ min. a Geo-Jack unconfined compression system was used to apply the load as shown in Figure 5.

Table 4. Solutions used for MICP treatment.

MICP Solution #1	MICP Solution #2	MICP Solution #3	MICP Solution #4
Deionized water	Urea medium	Urea medium	Urea medium
–	Cementation medium	Cementation medium	Cementation medium
–	–	Low concentration bacteria (1×10^8 cells/mL)	High concentration bacteria (2×10^8 cells/mL)

b. EICP Treatment

I. Sample preparation

Specimens prepared in the acrylic cell was used for EICP treatment. The preparation procedure of specimens was the same as that for MICP treatment. 957.7

g (2.1 lb) of BCS was mixed with 230 ml of one of the EICP solutions shown in Table 3 to achieve a targeted dry density of 96.1 pcf.

II. S-wave monitoring

Bender elements in the cell were connected to the data acquisition system after sample preparation. The readings of time difference on the oscilloscope were recorded every 15 minutes in the beginning. After the first three hours of treatment, the time difference was recorded every 12 hours until the end of the treatment period (3 days). The time difference readings were then used for calculating the S-wave velocities.

III. Unconfined compression test

After EICP treatment, specimens were extruded from the cell and dried in an oven for four days. Unconfined compression tests were performed for the specimens by following the same procedures for MICP treated specimens.

c. SEM and EDS Imaging

After unconfined compression tests of MICP-and EICP-treated specimens, some samples were collected from the fractured specimens and saved for Scanning Electron Microscope (SEM) and Electron Differential Spectrum (EDS) analysis. SEM images of samples were produced first to analyze the microscopic morphology of the samples. EDS was then used to scan the elements inside samples. The differences of SEM images and EDS analysis between the treated and the untreated samples were analyzed.

d. X-Ray Diffraction and Raman Spectroscopy

The X-Ray Diffraction (XRD) patterns were obtained using the Panalytical Empyrean X-Ray diffractometer (Cu Kα, λ=0. 154056 nm, 45 kV, 40 mA). The scattered radiation was detected in the angular range 5-60^{o} (2θ) with a scan rate of 4^{o}.min-1. The Raman spectra were recorded at an excitation wavelength of 532 nm. The spectra were scanned for 20 seconds in the range of 100-1400 cm^{-1} using Renishaw Invia Reflex Raman Microscope.

e. $CaCO_3$ Content

A carbonate analyzer chamber was used for the determination of $CaCO_3$ content as shown in Figure 6. A calibration line was first measured between $CaCO_3$ mass (g) and CO_2 pressure (kPa) before testing the specimens according to the ASTM specification (ASTM D4373-14). Samples were collected (20 to 50 g in mass) after each unconfined compression test. Each sample was weighed and placed into the carbonate analyzer chamber with a bucket filled with 8% HCl. The chamber was shaken to let HCl mix with the sample. Generated CO_2 pressure was recorded by the pressure gauge on top of the chamber. $CaCO_3$ content of the samples was calculated using measured CO_2 pressure based on the calibration line.

Discussion of Results

1. MICP-Treated BCS

a. Stainless Steel Cell Test

Figure 9 shows the variation of S-wave velocity versus time for MICP-treated BCS (BCS + Solution 3) and untreated BCS (BCS + Solution 2), as shown in Table 4. The S-wave velocity for MICP-treated BCS is 200 m/s lower than that of the untreated BCS. The S-wave velocities during loading and unloading stages are shown in Figure 10. The S-wave velocity did not show a substantial change during the loading and unloading stages for BCS-treated and untreated specimens. Figure 11 shows the settlement of the specimens during loading and unloading. The BCS-treated sample experienced a higher settlement than untreated specimens. The results of the S-wave velocities (Figure 9) and settlement (Figure 11) were contrary to what was expected,

Variations of the S-wave velocities of specimens treated by four MICP solutions (Table 4) are shown in Figure 12. S-wave velocities of MICP-treated BCS specimens were higher than the untreated specimen at the beginning of the MICP treatment. However, after 4 hours of the MICP treatment, untreated BCS samples had 150 m/s higher S-wave velocity than the MICP-treated BCS samples after 5 days. This is probably because MICP treatment may inhibit the lime hydration inside BCS. At the same time, $CaCO_3$ precipitation during MICP treatment was not adequate to improve the mechanical properties of BCS.

Figure 9. S-wave velocity versus time between untreated BCS and MICP-treated BCS.

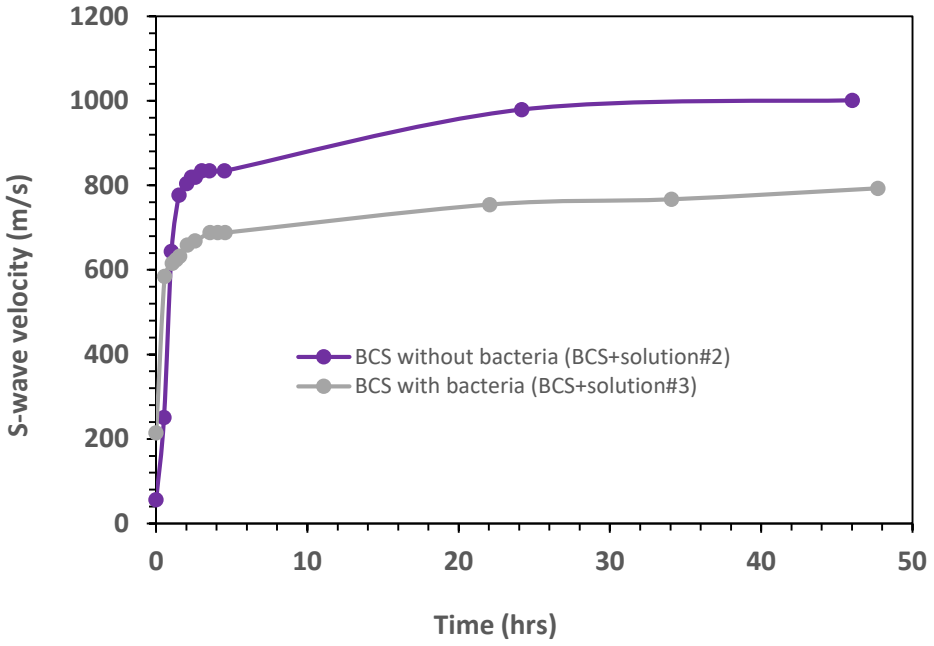

Figure 10. S-wave velocity of MICP-treated and untreated BCS during loading and unloading.

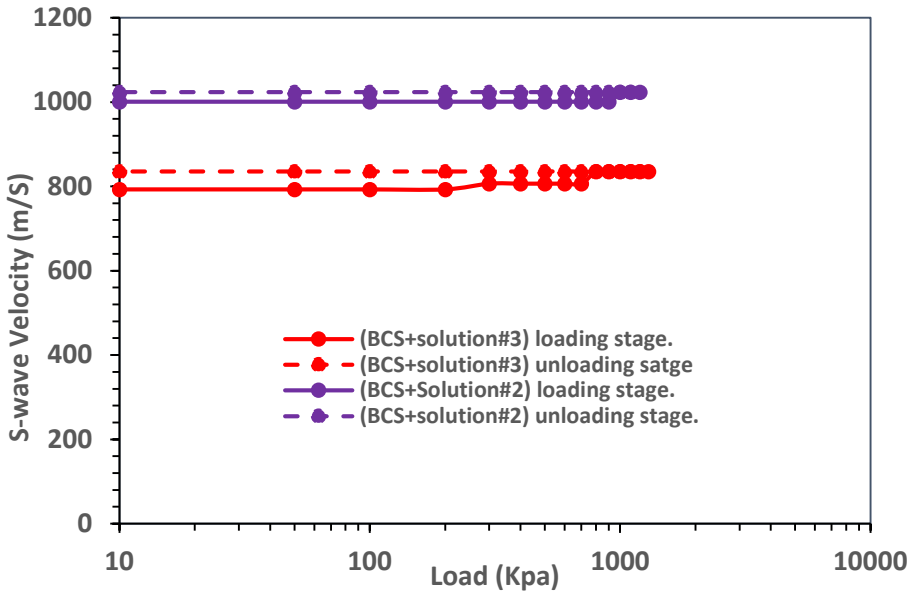

Figure 11. Settlement of MICP-treated and untreated BCS specimens.

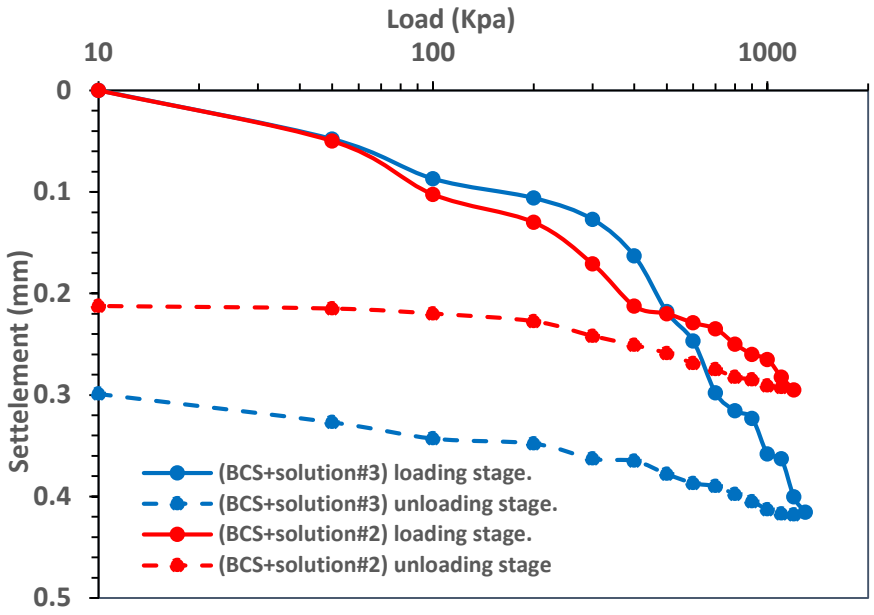

Figure 12. S-wave velocities versus time of BCS specimens treated by four different solutions.

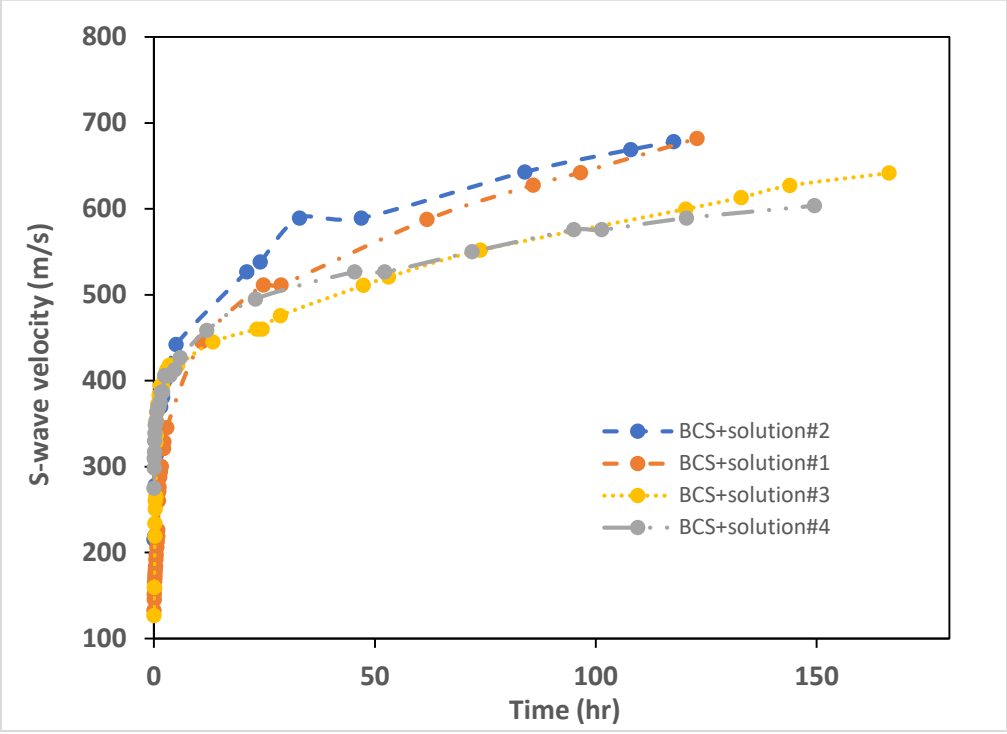

b. Unconfined Compression Test

S-wave signals measured in the acrylic cell specimens were not analyzed due to the cross-talk of the signals [36]. Unconfined compression test results of BCS with different solutions (Table 4) are shown in Figure 13. UCS of BCS mixed with deionized water has the highest compression strength and the BCS mixed with the bacteria has the lowest strength. The presence of SO_4 in BCS may work as a mineral growth inhibitor for $CaCO_3$ [40], which reduced the UCS of MICP-treated specimens.

c. $CaCO_3$ Content Measurement Chamber

Table 5 shows the average $CaCO_3$ content of untreated and MICP-treated BCS samples. $CaCO_3$ content was calculated by dividing the mass of $CaCO_3$ (measured by the $CaCO_3$ chamber test) by the mass of untreated BCS. The BCS samples treated with MICP had an average of 0.5 % $CaCO_3$ content.

d. SEM and EDS Imaging

The microscopic morphology of specimens is shown in Figure 14. Figure 14a shows BCS mixed with deionized water (i.e., Solution 1 in Table 4). Figure 14b shows BCS mixed with urea solution (i.e., Solution 2 in Table 4). Based on Figures 14a and b, there was not any $CaCO_3$ precipitation inside the samples. Figures 14c and d show BCS treated with MICP (i.e., Solution 3 and 4 in Table 4), which showed $CaCO_3$ precipitation on the surface of the particle, while, not at any particle contacts. Table 6 shows the results of EDS analysis, confirming the existence of $CaCO_3$ precipitation.

Figure 13. Unconfined compressive strength of BCS treated by different solutions.

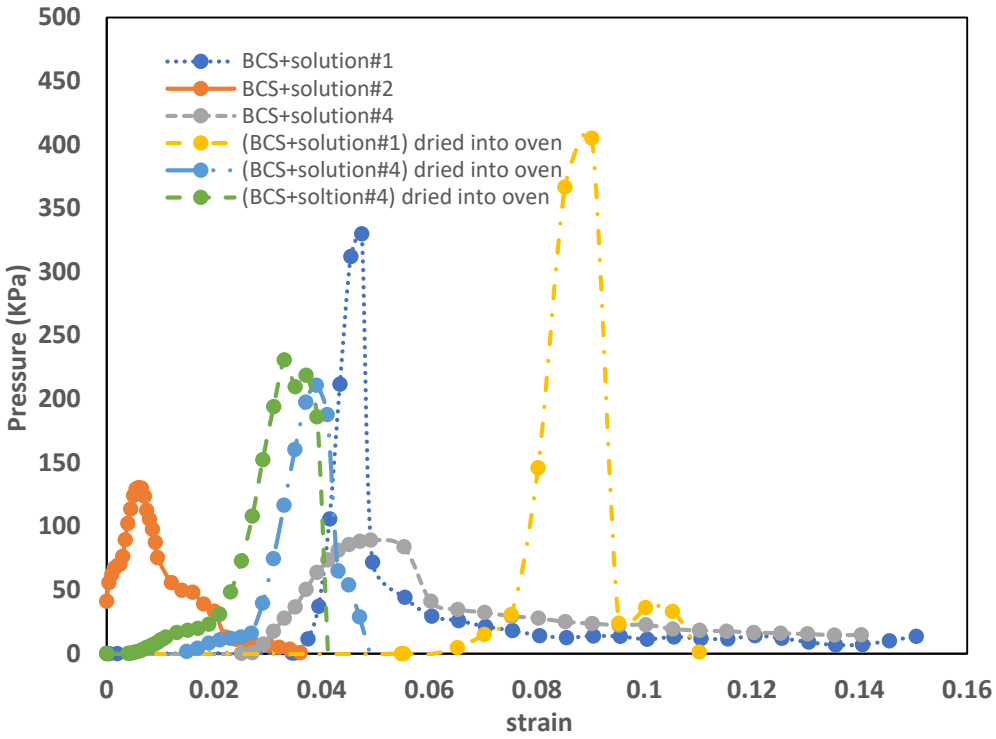

Table 5. $CaCO_3$ contents of BCS specimens treated by different MICP solutions.

Specimen	Weight of dry specimen (g)	Weight of $CaCO_3$ (g)	$CaCO_3$ (%)
BCS + solution #1	43.29	0.064	0.147
BCS + solution #2	29.04	0.028	0.097
BCS + solution #3	54.22	0.275	0.51
BCS + solution #4	52.5	0.275	0.527

Figure 14. SEM images of untreated and MICP-treated BCS specimens.

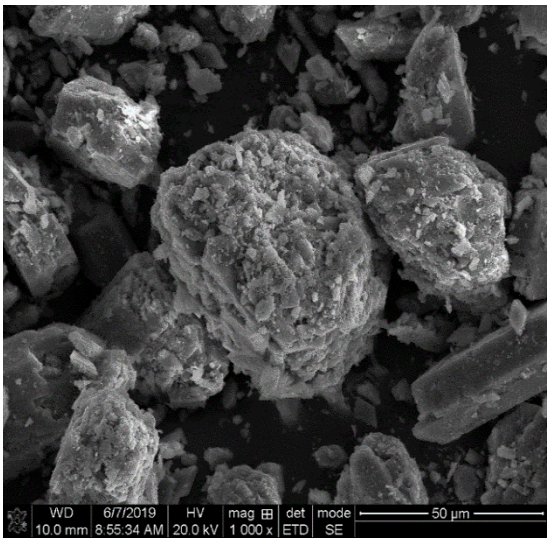

(a) BCS mixed with Solution 1 in Table 5

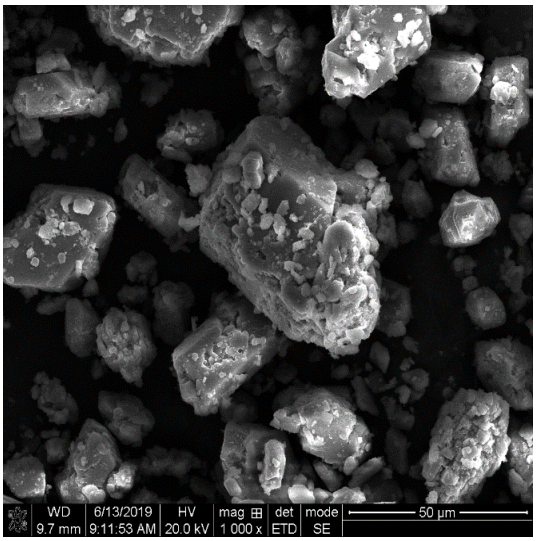

(b) BCS mixed with Solution 2 in Table 5

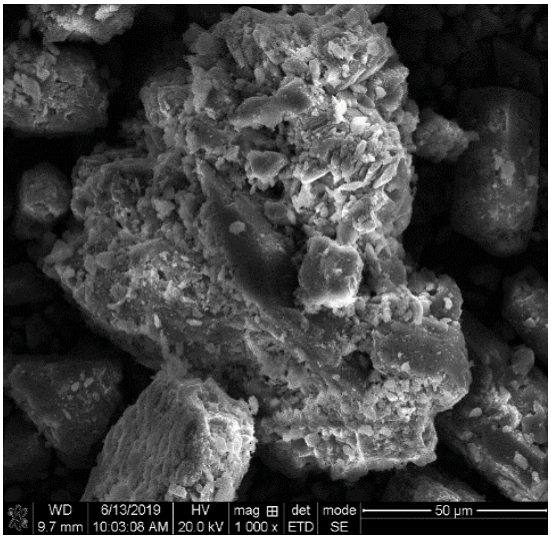

(c) BCS mixed with Solution 3 in Table 5

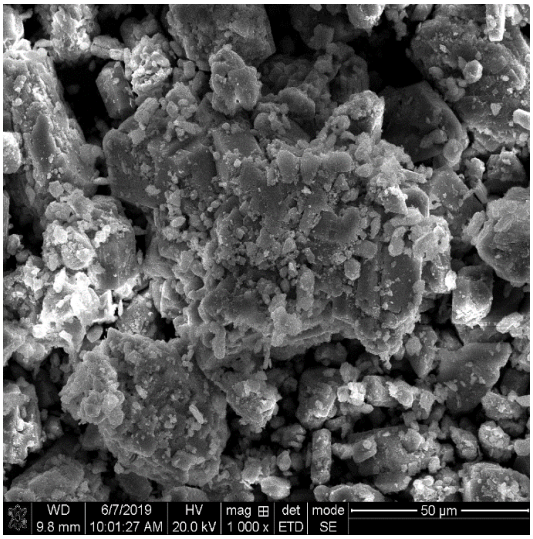

(d) BCS mixed with Solution 4 in Table 5

Table 6. Element composition (%) of MICP-treated and untreated BCS specimens.

Specimen	C	O	F	Al	Si	S	Ca	Fe	Cl	N
BCS + solution 1	1.2	30	1.73	1	0.83	26.03	39.86	0.23	--	--
BCS + solution 2	0.23	33.25	1.33	--	1.28	25.05	37.93	0.23	0.8	--
BCS + solution 3	0.64	30.36	1.7	0.32	1.46	23.18	40.46	1.3	0.64	0.64
BCS + solution 4	0.5	26.82	3.22	0.14	1.22	23.28	40.72	0.4	1.24	0.84

e. X-Ray Diffraction (XRD) and Raman Spectroscopy

Figures 15a and b show the XRD results of BCS and $CaCO_3$ minerals, respectively [22] [41]. Both figures were used as references to find the dominant crystals in untreated and MICP-treated BCS specimens. Figure 15c shows the XRD of the untreated BCS sample. The majority of the crystals in the specimen are shown, including gypsum, anhydrate, and quartz. Figure 15d shows the XRD of the MICP-treated BCS sample. The crystals in the specimen include gypsum, anhydrate, and calcite ($CaCO_3$).

Figure 16 shows the results of Raman spectroscopy. Figure 16a includes the standard Raman spectra for calcium sulfate hemihydrate and calcium sulfate dehydrate. Figure 16b shows the Raman spectrum of untreated BCS, which agrees with Raman spectra of calcium sulfate hemihydrate and calcium sulfate dehydrate in Figures 16a [42]. Figures 16c and d are Raman spectra of MICP-treated BCS samples treated by either low or high concentration of bacteria, which did not show agreement with Raman results of untreated BCS sample (Figure 16b) and thus demonstrated the existence of $CaCO_3$.

Figure 15. XRD spectra of untreated and MICP-treated samples.

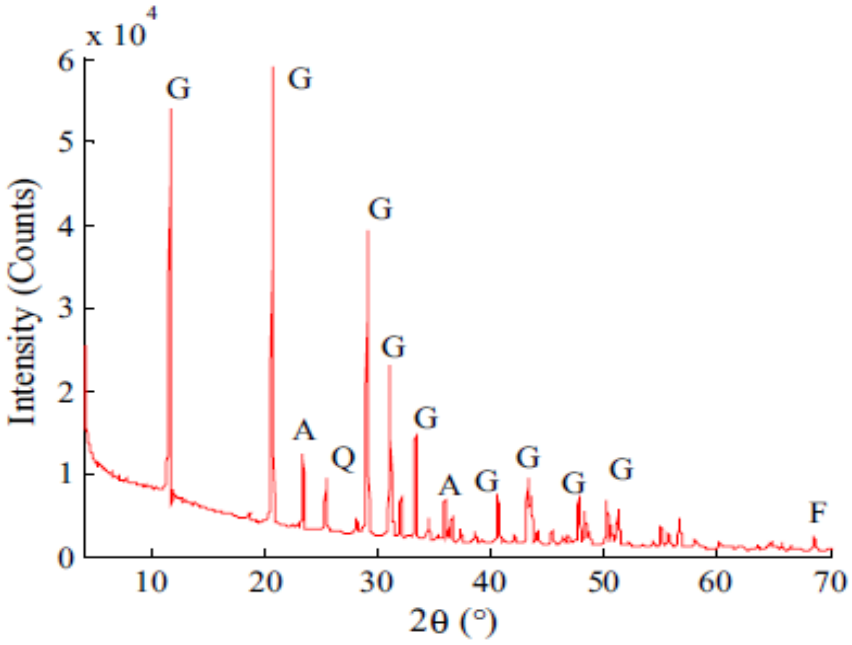

(a) XRD of a pH-adjusted FG sample (G: gypsum, A: anhydrate, F: fluorite, Q: quartz) [22]

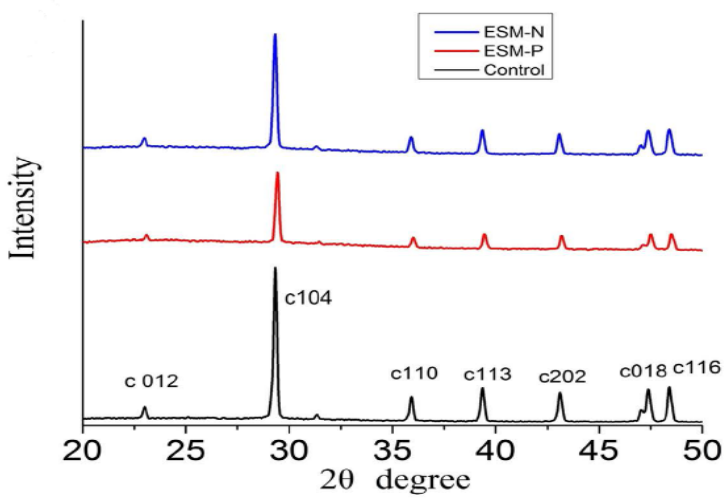

(b) XRD of the control sample, and $CaCO_3$ in the presence of ~2.5 μ g·mL−1 ESM-P and ESM-N proteins with 2θ degree from 20° to 50° [41]

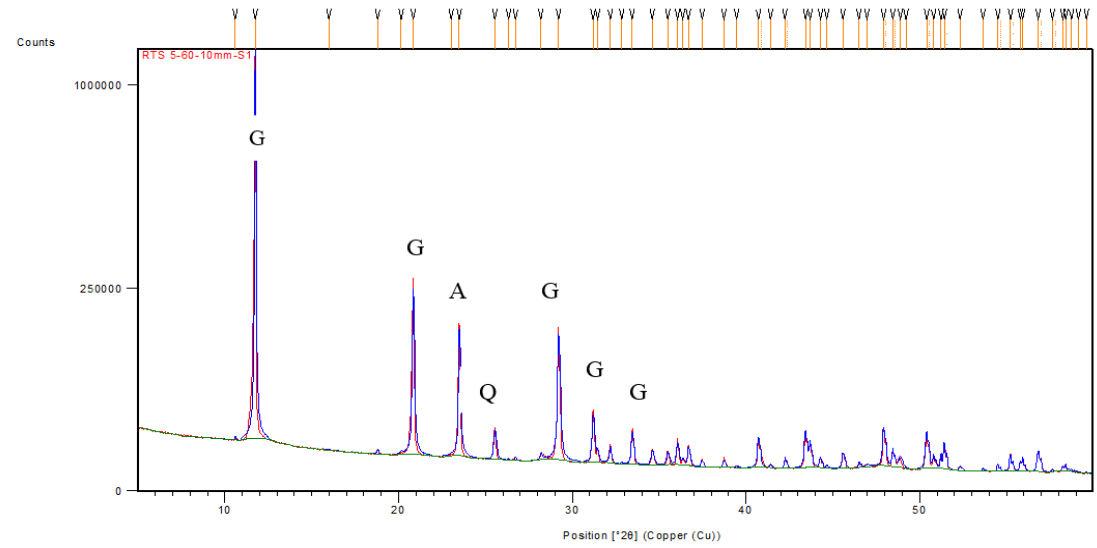

(c) XRD of untreated BCS (BCS+solution#1) (G: gypsum, A: anhydrate, Q: quartz).

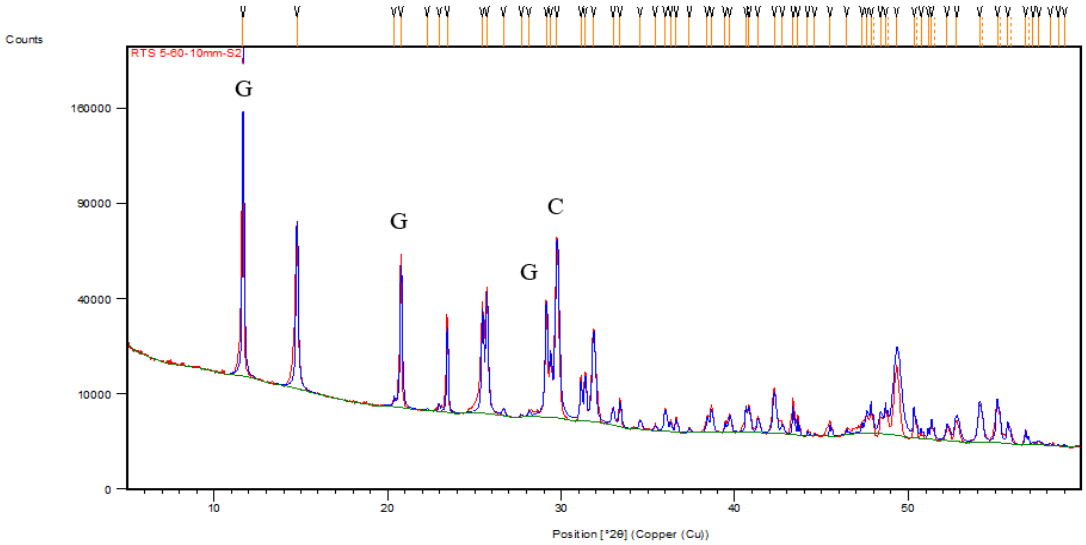

(d) XRD of MICP-treated BCS (BCS+solution#4) (G: gypsum, C: calcite).

Figure 16. Raman spectra of BCS Samples.

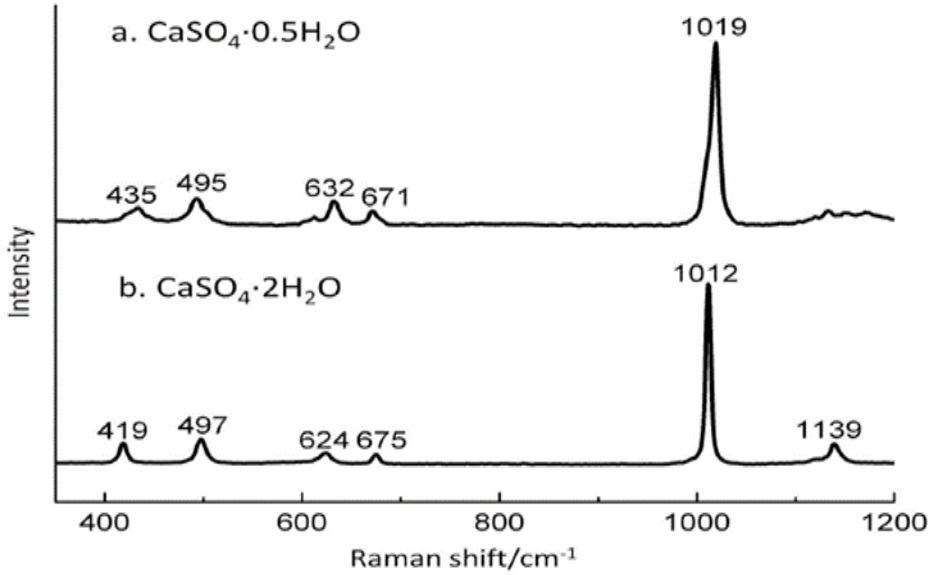

(a) Standard Raman spectrum of calcium sulfate hemihydrate ($CaSO_4.5H_2O$) and calcium sulfate dehydrate ($CaSO_4.2H_2O$) [42]

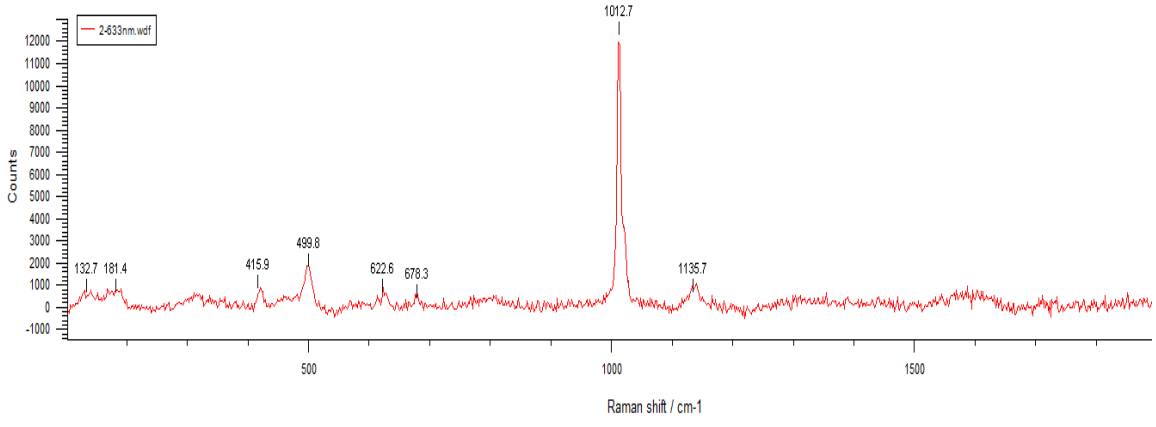

(b) Raman Spectrum of BCS+solution#1.

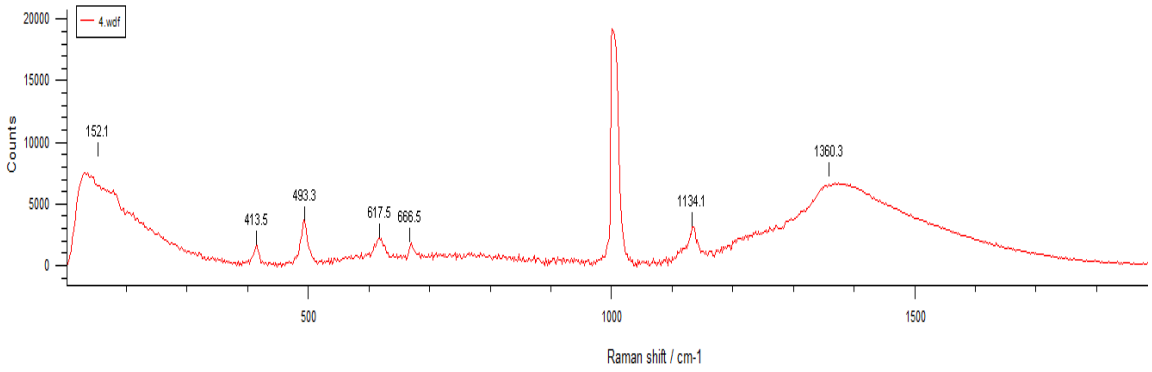

(c) Raman Spectrum of BCS+solution#3.

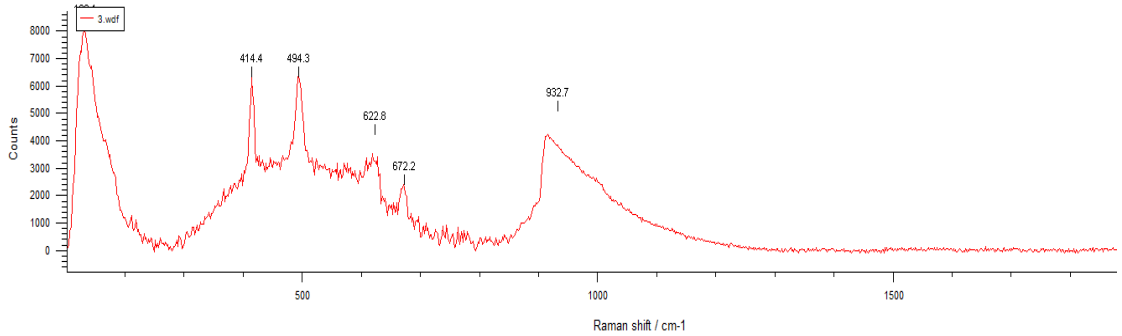

(d) Raman Spectrum of BCS+solution#4.

2. BCS-Treated by EICP

a. S-Wave Velocity

S-wave velocities of BCS specimens treated by different EICP solutions (Table 3) were measured after three days of curing time. Table 7 shows the S-wave velocities of three specimens. As shown in Table 7, there was no significant improvement of S-wave velocities of EICP-treated specimens (specimen No. 1 and 2) as compared to the untreated specimen (specimen No. 3). Furthermore, there was no significant difference between BCS treated with a mixture of enzyme and non-fat milk powder (specimen No. 1) and a mixture of enzyme only (specimen No. 2).

Table 7. S-wave velocity of BCS treated by different EICP solutions

Specimen	Ingredients	S-wave velocities after 3 days of curing (m/s)
1	BCS+EICP solution#1	532
2	BCS+EICP solution#2	511
3	BCS+EICP solution#3	487

b. Unconfined Compression Test

After EICP treatment, specimens were extracted from the acrylic cell. However, when extracting the specimens, specimens No. 1 and 2 were fractured immediately as shown in Figure 17. The observed fracture could be attributed to the wet condition inside the sample, which decreased their strength (i.e., water susceptibility). Therefore, unconfined compression tests were not performed.

Figure 17. EICP-treated BCS samples after extraction from the cell.

(a) Specimen No. 1: BCS+EICP solution#1

(b) Specimen No. 2: BCS+EICP solution#2

c. $CaCO_3$ Content

Table 8 shows the $CaCO_3$ content of three BCS specimens treated and untreated with EICP. Specimen No. 1 had the highest $CaCO_3$ content due to the stabilizing function of non-fat milk for the enzyme. Specimen No. 2 had a lower $CaCO_3$ content due to the absence of non-fat milk powder. Specimen No. 3 is a BCS specimen without mixing enzyme, which did not have an EICP reaction and has negligible $CaCO_3$ content.

Table 8. Average $CaCO_3$ contents of three untreated and EICP-treated BCS specimens

Specimen	weight of dry specimen (g)	$CaCO_3$ content (g)	$CaCO_3$ (%)
1	40.62	0.548	1.37
2	29.78	0.169	0.604
3	22.56	0.028	0.136

d. SEM and EDS Imaging

Fractured samples were used for SEM imaging and shown in Figure 18. BCS sample treated by the enzyme and non-fat milk (Figure 18a) apparently showed more $CaCO_3$ precipitation on the particle surfaces that that in the BCS sample treated only by the enzyme. Table 9 shows the results of EDS analysis, confirming specimen No. 1 had the highest $CaCO_3$ content.

Figure 18. SEM images of EICP-treated BCS.

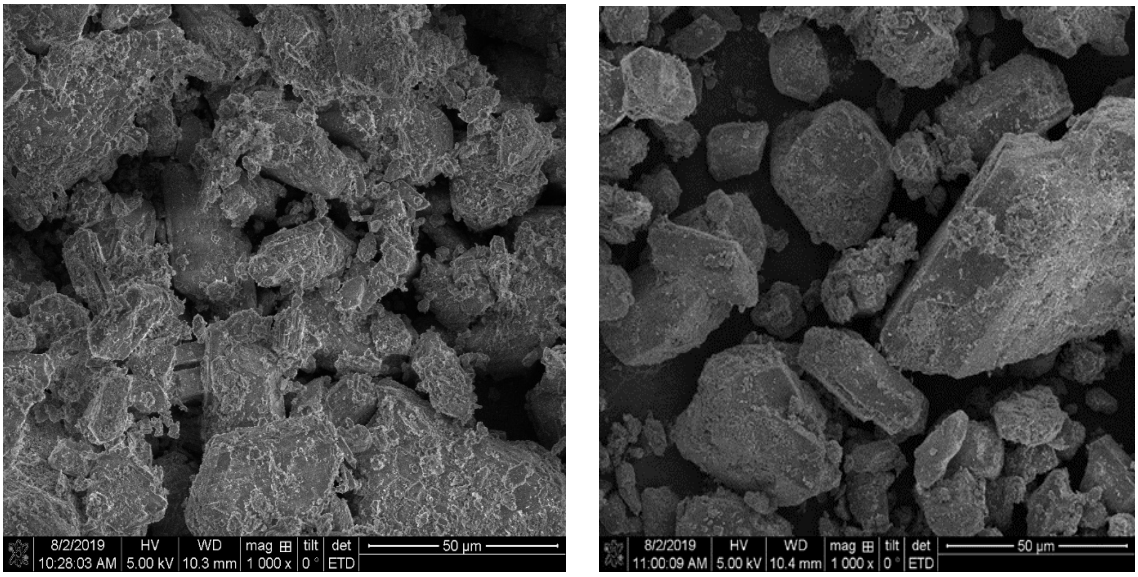

(a) BCS+EICP solution#1 (b) BCS+EICP solution#2

Table 9. The element composition (%) of untreated and EICP-treated BCS

Specimen	C	O	F	Al	Si	S	Ca	Fe	Cl
1	1.075	24.75	2.45	0.025	0.325	20.55	48.325	0.7	0.3
2	0.35	36.4	3.675	--	0.675	22.625	35.05	0.2	0.875
3	0.225	33.25	1.325	--	1.275	25.05	37.925	0.225	0.8

Conclusions

This research investigated the feasibility of stabilizing BCS using MICP and EICP treatments. The mechanical behavior of BCS after applying both treatments was investigated by measuring the S-wave velocities and performing unconfined compression tests. $CaCO_3$ content was measured. Microscale imaging and element analysis from SEM, EDS, XRD, and Raman analysis were presented to investigate the morphologies of particles and the presence of $CaCO_3$. Based on the data presented in this report, the following conclusions were drawn:

- Bender elements were used for monitoring MICP and EICP treatments. S-wave velocities of MICP-and EICP-treated BCS specimens were lower than untreated BCS specimens. This is probably because MICP and EICP treatments may inhibit the lime hydration inside BCS. At the same time, $CaCO_3$ precipitation during MICP and EICP treatments was not adequate to significantly improve the mechanical properties of BCS.
- $CaCO_3$ content measurements showed 0.52% of $CaCO_3$ content in the MICP-treated BCS specimens, 1.37% of $CaCO_3$ content in EICP-treated BCS specimens with enzyme and non-fat milk, and 0.6% of $CaCO_3$ content in EICP-treated BCS specimens with enzyme only. Although the presence of $CaCO_3$ in the treated BCS specimens was confirmed, it might not be enough and effective to cement the BCS particles together.
- SEM imaging and EDS analysis showed $CaCO_3$ precipitation inside the MICP-and EICP-treated samples. However, no cemented bond was observed between BCS particles, which may result in lower strength of MICP-and EICP-treated BCS specimens.
- Results of XRD and Raman spectroscopy of untreated BCS showed the standard spectrum of $CaSO_4$. $2H_2O$ (gypsum). XRD and Raman spectra confirmed the existence of $CaCO_3$ inside the MICP-and EICP-treated specimens.
- UCS of MICP-and EICP-treated specimens were lower than the UCS of untreated specimens. This is probably due to two reasons: (1) the presence of SO_4 (54% by weight) in BCS worked as a mineral growth inhibitor for $CaCO_3$ [40]. Dobberschütz (2018) [40] showed that the dominant mechanism for $CaCO_3$ inhibition was SO_4^{2-} ion adsorption, which blocks the growth sites and prevents attachment of $CaCO_3$ ion pairs; and (2) low pH of BCS may also inhibit $CaCO_3$ precipitation [15].

Recommendations

Based on the reported results, using MICP and EICP solutions is not an effective method for stabilizing BCS due to the presence of SO_4^{2-} and low pH of BCS that inhibit $CaCO_3$ precipitation. However, MICP and EICP could be effective for other geotechnical related applications, including sealing soil cracks on embankment slopes, ground improvement, and pile post-grouting [1], which is currently under investigation by the research team.

Acronyms, Abbreviations, and Symbols

Term	Description
λ	Spectrum wavelength
$CaCl_2$	Calcium Chloride
$CaCO_3$	Calcium Carbonate
$CO(NH)_2$	Urea
g.	gram(s)
H_2O	Water
Hz	hertz
L.	Liter(s)
M	Molarity concentration
m.	meter(s)
N.	Newton(s)
NH_4Cl	Ammonium Chloride
Pa.	Pascal
S.	Second(s)
U	Enzyme catalytic activity
V	Volt(s)

References

[1] H. Lin, M. T. Suleiman, H. M. Jabbour, D. G. Brown and E. Kavazanjian Jr, "Enhancing the axial compression response of pervious concrete ground improvement piles using biogrouting," *Journal of Geotechnical and Geoenvironmental Engineering,* vol. 142, no. 10, 2016.

[2] DeJong, J. T., M. B. Fritzges and K. Nüsslein, "Microbially induced cementation to control sand response to undrained shear," *Journal of Geotechnical and Geoenvironmental Engineering,* vol. 132, no. 11, pp. 1381-1392, 2006.

[3] Ivanov, Volodymyr, Chu and Jian, "Applications of microorganisms to geotechnical engineering for bioclogging and biocementation of soil in situ," *Reviews in Environmental Science and Bio/Technology,* vol. 7, no. 2, pp. 139-153, 2008.

[4] J. K. Mitchell and J. C. Santamarina, "Biological Considerations in Geotechnical Engineering," *131,* vol. 131, no. 10, pp. 1222-1233, 2005.

[5] Whiffin, V. S., L. A. V. Paassen and M. P. Harkes, "Microbial carbonate precipitation as a soil improvement technique," *Geomicrobiology Journal,* vol. 24, no. 5, pp. 417-423, 2007.

[6] S. G. J. K. a. B. S. S. Stocks-Fischer, "Microbiological precipitation of CaCO3," *Soil Biol Biochem,* vol. 31, p. 1563–1571, 1999.

[7] V. Paassen and L. Andreas, "Biogrout, ground improvement by microbial induced carbonate precipitation," 2009.

[8] H. Yasuhara, D. Neupane, K. Hayashi and M. Okamura, "Experiments and predictions of physical properties of sand cemented by enzymatically-induced carbonate precipitation," *Soils and Foundations,* vol. 52, no. 3, pp. 539-549, 2012.

[9] Hamdan and N. M, "Applications of enzyme induced carbonate precipitation (EICP) for soil improvement," 2015.

[10] A. Almajed, H. K. Tirkolaei and E. K. Jr, "Baseline investigation on enzyme-induced calcium carbonate precipitation.," *Journal of Geotechnical and Geoenvironmental Engineering,* vol. 144, no. 11, 2018.

[11] J. T. DeJong, K. K. Soga, B. S. E., V. Paassen and A. Q. L. A., "Biogeochemical processes and geotechnical applications: progress, opportunities and challenges," *Bio-and Chemo-Mechanical Processes in Geotechnical Engineering,* pp. 143-157, 2014.

[12] T. O'Donnell, Sean and E. K. Jr., "Stiffness and dilatancy improvements in uncemented sands treated through MICP.," *Journal of Geotechnical and Geoenvironmental Engineering,* vol. 141, no. 11, 2015.

[13] K. Feng and B. M. Montoya, "Influence of confinement and cementation level on the behavior of microbial-induced calcite precipitated sands under monotonic drained loading," *Journal of Geotechnical and Geoenvironmental Engineering,* vol. 142, no. 1, 2016.

[14] D. Terzis and L. Laloui, "3-D micro-architecture and mechanical response of soil cemented via microbial-induced calcite precipitation," *Scientific reports,* vol. 8, no. 1, pp. 1-11, 2018.

[15] Oliveira, P. J. Venda, L. D. Freitas and J. P. Carmona, "Effect of soil type on the enzymatic calcium carbonate precipitation process used for soil improvement," *Journal of Materials in Civil Engineering,* vol. 29, no. 4, 2017.

[16] Zhongjie Zhang, Mingjiang Tao, "Stability of Calcium Sulfate Base Coourse in a Wet Environment," LTRC, Baton Rouge, 2006.

[17] Mingjiang Tao, Zhongjie Zhang, "Enhanced Performance of Stabilized By-Product Gypsum," *Journal of Materials in Civil Engineering,* vol. 17, no. 6, pp. 617-623, November 2005.

[18] Chesner, W H, COLLINS, R J, MacKay, M H, "USER GUIDELINES FOR WASTE AND BY-PRODUCT MATERIALS IN PAVEMENT CONSTRUCTION," McLean, VA : U.S. Dept. of Transportation, Federal Highway Administration, Research and Development, Turner-Fairbank Highway Research Center ; [Springfield, Va.], McLean, VA, 1998.

[19] B. Christopher and V. C. McGuffey, Pavament subsurface drainage system, Transportation research board, 1997.

[20] K. Kovler, "Setting and hardening of gypsum-portland cement-silica fume blends, Part 1: temperature and setting expansion," *Cement and concrete research,* vol. 28, no. 3, pp. 423-437, 1998.

[21] K. Kovler, "Enhancing water resistance of cement and gypsum-cement materials," *Journal of materials in civil engineering,* vol. 13, no. 5, pp. 349-355, 2001.

[22] Y. Bigdeli and M. Barbato, "Development of new pH-adjusted fluorogypsum-cement-fly ash blends: Preliminary investigation of strength and durability properties," *Construction and Building Materials,* vol. 182, pp. 646-656, 2018.

[23] H. Lin, M. T. Suleiman, D. G. Brown and a. E. K. Jr., "Mechanical Behavior of Sands Treated by Microbially Induced Carbonate Precipitation," *Journal of Geotechnical and Geoenvironmental Engineering ,* vol. 142, no. 2, 2016.

[24] S. S. Bang, F. S., N. L. M. S. and B. L. Comes, "Application of novel biological technique in dust suppression," *Transportation research board,* pp. 09-0831, 2009.

[25] E. Kavazanjian Jr, E. Iglesias and I. Karatas., "Biopolymer soil stabilization for wind erosion control," *17th Int. Conf. Soil Mech. Geotech. Engng, Alexandria,* vol. 2, pp. 881-884, 2009.

[26] V. d. Ruyt, Michiel, Zon and a. W. v. der, "Biological in situ reinforcement of sand in near-shore areas," *Proceedings of the Institution of Civil Engineers-Geotechnical Engineering,* vol. 162, no. 1, pp. 81-83, 2009.

[27] M. Burbank and e. al., "Geotechnical tests of sands following bioinduced calcite precipitation catalyzed by indigenous bacteria," *Journal of Geotechnical and Geoenvironmental Engineering,* vol. 139, no. 6, pp. 928-936, 2013.

[28] B. M. Montoya, J. T. DeJong and a. R. W. Boulanger, "Dynamic response of liquefiable sand improved by microbial-induced calcite precipitation.," *Bio-and Chemo-Mechanical Processes in Geotechnical Engineering,* pp. 125-135, 2014.

[29] Jiang, Ning-Jun, K. Soga and M. Kuo, "Microbially induced carbonate precipitation (MICP) for seepage-induced internal erosion control in sand-clay mixtures," vol. 143, no. 3, 2017.

[30] K. M. Darby, G. L. Hernandez, J. T. DeJong, R. Boulanger, M. G. Gomez and D. W. Wilson, "Centrifuge model testing of liquefaction mitigation via microbially induced calcite precipitation," *Journal of Geotechnical and Geoenvironmental Engineering,* vol. 145, no. 10, 2019.

[31] J. Do, B. M. Montoya and a. M. A. Gabr, "Simulated implementation approach for microbially induced carbonate precipitation improvement of soil adjacent to piles," *Geo-Congress 2019: Soil Improvement,* pp. 280-288, 2019.

[32] S. Safavizadeh, B. M. Montoya, Gabr., A. and Mohammed, "Microbial Induced Calcium Carbonate Precipitation in Coal Ash.," *Géotechnique,* vol. 69, no. 8, pp. 727-740, 2019.

[33] P. Bick, H. Bastola, M. T. Suleiman, J. Gu, P. Diplas, D. G. Brown and N. Zouari, "Minimizing Wind Erosion using Microbial Induced Carbonate Precipitation".

[34] D. Neupane, H. Yasuhara, N. Kinoshita and T. Unno., "Applicability of enzymatic calcium carbonate precipitation as a soil-strengthening technique," *Journal of Geotechnical and Geoenvironmental Engineering,* vol. 139, no. 12, pp. 2201-2211, 2013.

[35] A. Nafisi, S. Safavizadeh and B. M. Montoya, "Influence of Microbe and Enzyme-Induced Treatments on Cemented Sand Shear Response," *Journal of Geotechnical and Geoenvironmental Engineering,* vol. 145, no. 9, 2019.

[36] J.-S. Lee and J. C. Santamarina., "Bender elements: performance and signal interpretation," *Journal of geotechnical and geoenvironmental engineering,* vol. 131, no. 9, pp. 1063-1070, 2005.

[37] ASTM., "Standard test method for rapid determination of carbonate content of soils.," *American Socity of Testingof Materials,* 2014.

[38] A. e. a. Almajed, "Enzyme induced biocementated sand with high strength at low carbonate content," *Scientific reports,* vol. 9, no. 1, pp. 1-7, 2019.

[39] T. S. Yun and J. C. Santamarina, "Decementation, softening, and collapse: changes in small-strain shear stiffness in k 0 loading," *Journal of Geotechnical and Geoenvironmental engineering,* vol. 131, no. 3, pp. 350-358, 2005.

[40] D. Sören, M. R. S. K. Nielsen, C. K., B. R., N. and M. P. Andersson, "The mechanisms of crystal growth inhibition by organic and inorganic inhibitors," vol. 9, no. 1, pp. 1-6, 2018.

[41] C. Liu, L. Xie and R. Zhang., "Heterogeneous distribution of dye-labelled biomineralizaiton proteins in calcite crystals," *Scientific reports,* vol. 5, no. 1, pp. 1-8, 2015.

[42] Y. W. Wang, Y. Y. Kim, H. K. Christenson and F. C. Meldrum, "A new precipitation pathway for calcium sulfate dihydrate (gypsum) via amorphous and hemihydrate intermediates," *Chemical Communications,* vol. 48, no. 4, pp. 504-506, 2011.

[43] V. Zahavi and J. M. Ryan, "Stability of Travel Over Time," *Transportation Research Record 750,* p. 70–75, 1980.

[44] T. Lind, "Ash formation in circulating fluidised bed combustion of coal and solid biomass," *Technical Research Centre of Finland,* 1999.